

## Effects of Solution pH and Surface Chemistry on the Postdeposition Growth of Chemical Bath Deposited PbSe Nanocrystalline Films

Shaibal K. Sarkar,<sup>†</sup> Shifi Kababya,<sup>‡</sup> Shimon Vega,<sup>‡</sup> Hagai Cohen,<sup>§</sup> Joseph C. Woicik,<sup>||</sup>  
Anatoly I. Frenkel,<sup>⊥</sup> and Gary Hodes<sup>\*,†</sup>

Departments of Materials and Interfaces, Chemical Physics, and Chemical Research Support, Weizmann Institute of Science, Rehovot 76100, Israel, National Institute of Standards and Technology, Gaithersburg, Maryland 20899, and Physics Department, Yeshiva University, New York, New York 10016

Received March 15, 2006. Revised Manuscript Received December 8, 2006

Chemical bath deposited PbSe films were subjected to postdeposition treatment with aqueous (typically 0.25–0.5 M) KOH. For films deposited using a citrate complex, this treatment resulted in dissolution of surface lead oxides (seen from XPS and EXAFS measurements) and growth of the nanocrystals (from ca. 5 to as much as 20 nm, measured by XRD and TEM) by an Ostwald ripening mechanism and formation of a porous network. For films deposited using KOH-complexed Pb, this growth did not occur. The latter films are made up of PbSe crystals (ca. 4 nm) embedded in an amorphous matrix of lead oxide. Successful etching of the crystallite surface passivation is found to be critical for the growth progress. While the KOH treatment removed most of this matrix, the individual crystals of PbSe still remained passivated with a surface where Pb was apparently bonded to both O and Se. With use of a concentrated KOH solution (3 M) for long periods of time (>1 h), this surface could be removed and crystal growth occurred to give a network of PbSe crystals several tens of nanometers in size. This study, besides explaining the very different chemical behaviors of the two types of PbSe films, demonstrates the important role of what appear to be small differences in surface chemistries in determining the chemical properties of nanocrystals.

### Introduction

PbSe quantum dots (QD) exhibit size quantization at relatively large crystal size (smaller than ca. 70 nm) due mainly to the small reduced effective electron/hole mass and, to a lesser extent, to the high dielectric constant which screens the electron/hole Coulomb interaction (this interaction opposes the charge localization). Films of PbSe have been deposited by chemical bath deposition (CBD) since 1949<sup>1</sup> (actually earlier, but this earlier literature was classified due to wartime consideration of the PbSe films as IR detectors). More recently, quantum size effects in CBD PbSe films have been reported.<sup>2–5</sup> Control over the degree of size quantization depends on the ability to control the crystal size. Crystal size depends on many solution parameters. Not surprisingly, increase in deposition temperature leads to an increase in crystal size. However, another important parameter is the degree of complexation of the metal ion, which is a function of the strength of the complex for the particular metal ion used and the complexant to metal ion concentration ratio, which determines the presence or absence of a (hydr)oxide colloid in the starting solution.<sup>5–7</sup>

In our investigation of these PbSe films, we noted that the crystal size of the PbSe in films deposited from a citrate complexing bath could be considerably increased simply by immersing the films in an aqueous solution of relatively high pH (pH  $\geq$  12). On the other hand, films deposited from a hydroxide complexing bath, where the pH was ca. 14 (higher than the pH of solutions which increased the crystal size of citrate-deposited films), resulted in very small crystals (4 nm).<sup>5</sup> This apparent inconsistency was (partly) solved when we found that films deposited from the hydroxide bath did not grow further when immersed in a solution of high pH, contrary to films deposited from the other complexants. This observation suggested a different surface chemistry for the two types of films.

This paper describes these phenomena in detail and seeks to explain them. We show that the crystal growth at high pH can be explained by an Ostwald ripening mechanism involving dissolution and reprecipitation of PbSe. Using NMR and XPS to study the surface chemistry of the various PbSe samples, we find that the citrate-complexed films consist of tightly packed PbSe nanocrystals, where the nanocrystal surfaces are oxidized. The hydroxide-complexed films, on the other hand, are made up of isolated PbSe nanocrystals surrounded by a matrix which is predominantly a hydrated oxide of Pb. KOH postdeposition treatment of the hydroxide-complexed films removes most of this matrix;

\* To whom correspondence should be addressed. E-mail: gary.hodes@weizmann.ac.il.

<sup>†</sup> Department of Materials and Interfaces, Weizmann Institute of Science.

<sup>‡</sup> Department of Chemical Physics, Weizmann Institute of Science.

<sup>§</sup> Department of Chemical Research Support, Weizmann Institute of Science.

<sup>||</sup> National Institute of Standards and Technology.

<sup>⊥</sup> Yeshiva University.

(1) Milner, C. J.; Watts, B. N. *Nature* **1949**, *163*, 322.

(2) Biró, L. P.; Darabont, A.; Fitori, P. *Europhys. Lett.* **1987**, *4*, 691.

(3) Dadarlat, D.; Candea, R. M.; Turcu, R.; Biro, L. P.; Zaslavitskii, I. I.; Valeiko, M. V.; Shotov, A. P. *Phys. Status Solidi A* **1988**, *108*, 637.

(4) Hodes, G.; Albu-Yaron, A. *Proc. Electrochem. Soc.* **1988**, *88-14*, 298.

(5) Gorer, S.; Albu-Yaron, A.; Hodes, G. *J. Phys. Chem.* **1995**, *99*, 16442.

(6) Gorer, S.; Hodes, G. *J. Phys. Chem.* **1994**, *98*, 5338.

(7) Gorer, S.; Albu-Yaron, A.; Hodes, G. *Chem. Mater.* **1995**, *7*, 1243.

however, for crystal growth to occur, a much more aggressive hydroxide treatment is needed.

Quantitative information about the changes in the chemical composition between the samples before and after their KOH postdeposition treatment was obtained by extended X-ray absorption fine-structure (EXAFS) measurements. EXAFS results, obtained separately for Pb and Se local environments in these samples, were in excellent agreement with conclusions made from other techniques used in this study.

## Experimental Section

**PbSe Film Deposition.** PbSe films were deposited by chemical bath deposition (CBD). Lead acetate was complexed using either trisodium citrate (TSC films) or hydroxide (KOH films). Sodium selenosulfate ( $\text{Na}_2\text{SeSO}_3$ , prepared by refluxing 0.2 M Se powder with 0.5 M  $\text{Na}_2\text{SO}_3$  at ca. 80 °C for several hours) was used as the Se source. For the films grown with TSC complex, the final solution composition was 60 mM  $\text{Pb}^{2+}$ , 50 mM  $\text{Na}_2\text{SeSO}_3$ , and 160 mM TSC at a pH of ca. 10.5. For the KOH-complexed films, the solution composition was 60 mM  $\text{Pb}^{2+}$ , 50 mM  $\text{Na}_2\text{SeSO}_3$ , and 0.6 M KOH at a pH > 13. The Pb solution is first slowly added to a stock KOH solution (we used 0.5 M  $\text{PbAc}_2$  and 2 M KOH stock solutions). If the KOH is added to the  $\text{PbAc}_2$ , a white precipitate forms which does not readily redissolve on addition of more KOH. Film thicknesses were typically 40–50 nm, deliberately limited to a thickness where TEM could readily be carried out. Details of the deposition conditions, mechanisms, and further characterizations were reported elsewhere.<sup>1</sup> Under the conditions used here, the deposition proceeded through a cluster mechanism, whereby the selenosulfate reacted with a colloidal “ $\text{Pb}(\text{OH})_2$ ” (possibly a hydrated oxide) to form PbSe. We note that the age of the selenosulfate solution is often important in PbSe deposition. Fresh selenosulfate often results in rapid precipitation of PbSe when the selenosulfate solution is added. We find it more reproducible and controllable to use a selenosulfate solution which has been aged for about 2 days. (The activity of the solution changes rapidly in the first couple of days after preparation and then much more slowly; it can safely be used for several weeks after preparation with no special storage precautions, although it does slowly deactivate continuously, with increasing precipitation of black Se. In this study, the maximum age of the selenosulfate solutions was 8 days.) Samples for XRD and TEM were deposited on glass microscope slides. For XPS, depositions were on 60 nm thick gold-coated microscope glass substrates.

**KOH Treatment.** As-deposited films were treated with various concentrations of KOH in water (unless another solvent was specifically mentioned) for times up to 40 min. If not specified otherwise, the standard treatment was in 0.25 M KOH for 30 min. A more aggressive treatment (3 M KOH for 70 min) was used for the KOH films where specified.

**Sample Characterization.** XRD measurements on the films were carried out using a Rigaku RU-200B Rotaflex powder diffractometer with a grazing angle thin film measurement accessory operating in the  $\theta$ – $2\theta$  Bragg configuration or simple  $2\theta$  grazing angle (angle of incidence = 5°) configuration using Cu K $\alpha$  radiation. From the XRD peak broadening, grain sizes were calculated by the Scherrer formula.

TEM measurements were used to determine crystal size and film morphology. Samples were prepared by scraping the films from the glass substrates and floated onto TEM grids from water. TEM bright field imaging, EDAX, and EELS measurements were performed with a Phillips CM120 or a FEI Tecnai F30 microscope, operating at 120 and 300 kV, respectively.

XPS measurements were performed on a Kratos AXIS-HS setup, using a monochromatic Al K $\alpha$  source at 75 W. Efficient reduction of charging effects was achieved by applying a biased grid above the sample, as indicated by the agreement in line positions (e.g., Au, Pb, Se) with literature data. Repetitive scans were applied for the study of beam-induced effects, whereas the data shown below correspond to damage-free surfaces.

For the NMR analyses, since larger amounts of material were required than obtainable from the films, precipitates (TSC samples and KOH samples), which formed in parallel with the films deposition, were collected and thoroughly rinsed with water. The main XPS spectral features of the films, which are very different for the TSC and KOH depositions (see Results and Discussion) are reflected in the corresponding precipitates: therefore, we believe the unavoidable use of precipitates rather than films is justifiable. One of the TSC samples was treated with a 0.25 M KOH solution for 15 min. Weight measurements were carried out using a Mettler AE240 balance, measuring to 10  $\mu\text{g}$ . Due to variations between measurements, probably mainly in moisture uptake, we conservatively estimate the measurement precision to be better than 0.3 mg.

<sup>1</sup>H and <sup>13</sup>C NMR experiments were performed on a DSX-300 Bruker spectrometer operating at 300.15 and 75.47 MHz, respectively. A magic angle, 4 mm double resonance, spinning probe was used at ambient temperature. The spinning rate was 10 and 5 kHz during the <sup>1</sup>H and <sup>13</sup>C experiments, respectively. MAS (magic angle spinning) NMR spectra of <sup>1</sup>H were obtained after four accumulations of echo experiments with  $\pi/2$  and  $\pi$  pulses of 3 and 6  $\mu\text{s}$ , an echo delay of 100  $\mu\text{s}$ , and repetition delays of 10 s. All spectra were deconvoluted using the dmfit<sup>8</sup> computer program.

<sup>13</sup>C MAS spectra were recorded using cross-polarization CPMAS experiments followed by echo detection. The Hartman-Hahn matching conditions were set around 50 kHz and the CP mixing time was 5 ms. The echo delay after the cross-polarization was 200  $\mu\text{s}$  and a repetition time of 6 s was used. Proton decoupling was employed with an irradiation strength of 80 kHz. The number of signal accumulations necessary for obtaining a sufficient signal-to-noise (S/N) value was 11000. The <sup>13</sup>C chemical shifts were referred to 0 ppm for the single TMS line.

EXAFS measurements were performed at the UNICAT beamline facility 33BM at the Advanced Photon Source. Se K and Pb L<sub>3</sub> absorption edge data were recorded by collecting either the Se K or Pb L<sub>3</sub> fluorescence emission as a function of photon energy and normalizing to the incident photon flux as recorded by a N<sub>2</sub>-filled ion chamber upstream of the sample. Data were collected both before and after immersing the samples in 0.25 M KOH solution for 10 min.

## Results and Discussion

**XRD of TSC and KOH Films before and after KOH Treatment.** The effect of the KOH treatment on as-deposited (from a TSC bath at 35 °C) PbSe films is shown in Figure 1. Figure 1a shows the XRD spectrum of an as-deposited PbSe film. The average as-deposited crystal size estimated from the peak broadening is 5.5 nm. Treatment of the films with various concentrations of KOH (for 15 min) results in growth of the crystal size up to ca. 20 nm (Figures 1b–1f). The growth is strongly dependent on the KOH concentration up to ca. 0.25 M and then levels off gradually at higher concentrations.

(8) Massiot, D.; Fayon, F.; Capron, M.; King, I.; Le Calvé, S.; Alonso, B.; Durand, J.-O.; Bujoli, B.; Gan, Z.; Hoatson, G. *Magn. Reson. Chem.* **2002**, *40*, 70.

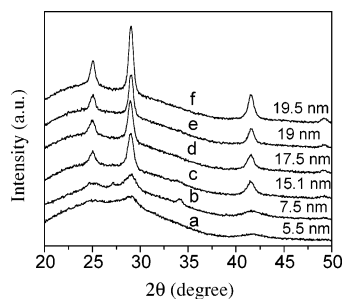


**Figure 1.** XRD spectra of TSC PbSe films as deposited (a) and after 15 min of treatment with aqueous KOH solutions of the following concentrations: 0.125 M (b); 0.25 M (c); 0.5 M (d); 1 M (e); 2 M (f). The crystal sizes, estimated from the peak widths, are given in the figure.

Films deposited from KOH baths (where the bath pH was ca. 14) exhibited no XRD spectrum, both before and after hydroxide treatment. However, as will be seen later (in the TEM study), no change in crystal size occurred for these films after the KOH treatment.

To understand this pronounced difference between the TSC and KOH films, as well as to understand the effect of the KOH treatment on the TSC films, we carried out a comprehensive characterization of both types of films before and after KOH treatment, using TEM, XPS, and NMR, and in some cases, EXAFS.

#### TEM of TSC Films before and after KOH Treatment.

We had previously reported that PbSe films deposited from TSC baths, in the regime where the cluster mechanism dominates (contrary to films grown via the ion-by-ion mechanism, where the crystal size was much larger), consist of PbSe nanocrystals embedded in an apparent amorphous matrix.<sup>7</sup> We had assumed that this matrix was amorphous PbSe based on preliminary EDX microprobe measurements, which showed no difference in composition between the crystalline (which by lattice imaging was shown to be PbSe) and amorphous regions.<sup>7</sup> Figures 2a and 2b show TEM images of an as-deposited TSC bath PbSe film at two different magnifications. The presence of what we considered to be the matrix can be clearly seen, particularly in the lower magnification image. However, under HRTEM, examining fixed regions of the samples under different conditions of focusing, we found that essentially the entire image was composed of crystals (if one region appeared amorphous at a certain focus depth, it was visibly crystalline at a different depth). EELS measurements using high-resolution imaging again showed no reproducible difference in composition between the two regions, as did EDS in our earlier work.<sup>7</sup>

Thus, we are now led to the conclusion that what we thought to be amorphous material is, in fact, crystalline PbSe. The crystals tend to be somewhat irregular and often elongated, with a typical overall size of ca. 5 nm.

After KOH treatment, the crystals grow from typically 5 nm to a porous, interconnected lattice of crystals typically  $10 \times 20$  nm in size (Figure 2c).

#### XPS of TSC Films before and after KOH Treatment.

XPS shows important differences between the as-deposited TSC films and the same films after KOH treatment. Figure 3 shows the Pb and Se XPS spectra of these two films. Semiquantitative data (including C and O peaks) are given in Table S1 (Supporting Information). Looking first at the

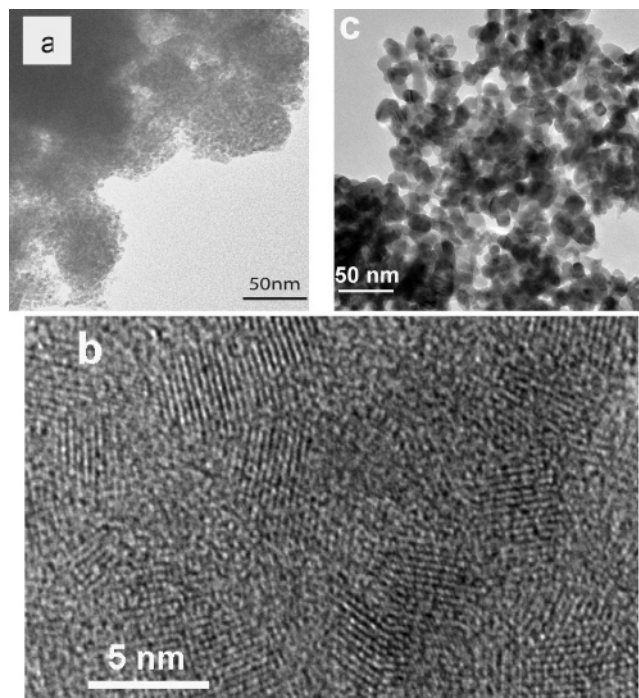


**Figure 2.** TEM micrographs of TSC PbSe films as-deposited ((a) and (b) at two different magnifications) and after KOH treatment (c).

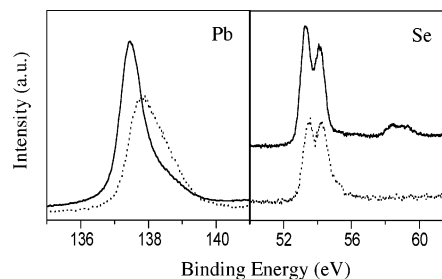


**Figure 3.** XPS spectra of Pb (left) and Se (right) of TSC PbSe both as-deposited (dotted lines) and after KOH treatment (solid lines).

Pb spectrum of the as-deposited film, it can be decomposed into two different lines representing two different Pb species (the decompositions of this and other lines are not shown here as they would make the figures very complicated and difficult to comprehend). The low BE line (ca. 137.5 eV) can be assigned to the Pb in PbSe. The higher BE line (ca. 138.3 eV) is associated with either a Pb–O bond (an oxide or hydrated oxide) or a Pb–CO bond (citrate or carbonate from atmospheric CO<sub>2</sub>). The C spectrum of the as-deposited film (not shown) contains a small peak at 289 eV which can be attributed to the carboxylate species. The Se spectrum consists of three doublets with the 3d<sub>5/2</sub> line at 53.4, 54.18, and 55.62 eV. The 53.4 peak (the main one) can be attributed to Se in PbSe. The higher BE peaks are attributed to Se, bound to Pb within a partially oxidized environment, e.g., neighboring Pb–O or other O-containing species (to be discussed in more detail in the Model section). In what follows, we refer to these Se peaks as Se(Pb-ox). [In ref 9, a broad Se peak was deconvoluted into a peak at 53.7 eV and another at 54.3, attributed to the 3d<sub>5/2</sub> and 3d<sub>3/2</sub> states, respectively. In our case, we clearly resolve the same broad peak and, from the deconvolution, see clear evidence for different chemical species of Se.] The small peak at 55.6 eV could also conceivably originate from elemental Se co-

deposited with the PbSe. The selenosulfate solution is an equilibrium between the selenosulfate ion and elemental Se and sulfite ion, and colloids of elemental Se may be present to a greater or lesser extent in the deposition solution.

After the KOH treatment, the spectra change markedly. The higher BE Pb–(C)O peak is strongly reduced and the spectrum is now dominated by the PbSe peak (see also the quantitative data in Table S1, Supporting Information).

The fact that the 289 eV C peak, formerly attributed to citrate, is strongly reduced after the KOH treatment (Table S1), together with the nature of the KOH treatment, suggests that the remaining oxidized (higher BE) Pb peak in the KOH-treated film is predominantly due to a Pb–O linkage. From the Se spectrum after treatment, it is seen that the Se(Pb-ox) peaks are much smaller. The broad peak centered on 59 eV is oxidized Se (e.g., SeO<sub>2</sub> and PbSeO<sub>x</sub>) which is often seen on the surface of selenides due to air oxidation (e.g., see ref 9). The apparent increase in the Se 3d<sub>5/2</sub> peak at ca. 53.3 eV is due to removal of the Se(Pb-ox) component which overlaps with the Se 3d<sub>3/2</sub> from the PbSe. The KOH treatment reduces the overall O concentration and transforms a large part of the main line (531.3 eV) to a lower BE (530.3 eV).

Quantitative elemental analyses from the XPS spectra are shown in Table SI in the Supporting Information. (EDS and EELS compositional analyses were carried out on some films in parallel to the XPS analyses, with essentially identical results.) In all cases, there appears to be excess Pb compared to Se. The Pb:Se ratio of the as-deposited TSC film is 2.0. The contribution from the higher BE peak at 138.3 (Pb–O or Pb–CO) is almost 50% greater than that from the lower BE peak at 137.7 (PbSe) (in spite of the smaller peak height of the higher BE peak, it is considerably broader than the low BE one). The ratio between the Pb peak arising from PbSe and the total Se peaks is 0.86. We consider this sufficiently close to unity particularly as there may be Pb atoms with both O and Se linkages, meaning some of the Pb contributing to the Pb–O peak may also be bonded to Se. The higher BE Pb peak was assumed, as discussed above, to be bonded to O or C (the O as oxide or hydrated oxide and the C as citrate or carbonate; the latter could form from dissolved CO<sub>2</sub>). The carboxylate C peak (at 289 eV) is relatively small and most of the C is from another source. The high BE Pb:O ratio is 0.46. Assuming that part of the O originates from the citrate (deduced from the carboxylate C peak), this ratio changes to ca. 0.5, which could cover a range of different oxides/hydrated oxides/basic carbonates.

We conclude that the films are composed of PbSe crystals covered predominantly with Pb-oxide/hydroxide and some adsorbed citrate.

After KOH treatment, the Pb:Se ratio drops to 1.3, which is much closer to the ratio of stoichiometric PbSe. Lattice imaging also shows that most of the deposit is PbSe. There is probably some Pb–O or Pb–CO left at the surface (also Pb–SeO<sub>x</sub>), although the intensity of the corresponding Pb peak is higher than can be explained by a single-atom surface shell.

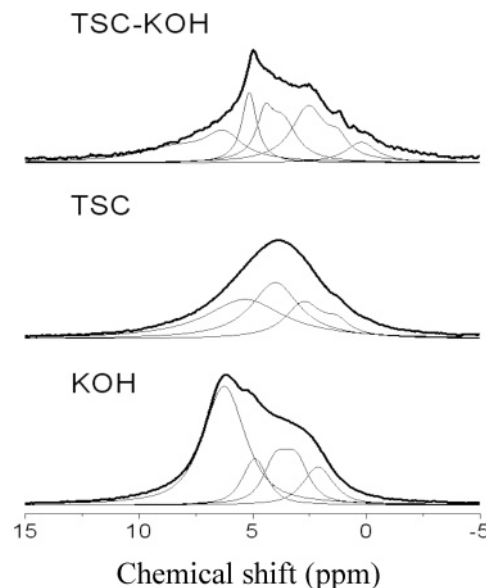


**Figure 4.** Room temperature <sup>1</sup>H MAS spectra of PbSe precipitates: TSC (as-deposited), KOH-treated (TSC-KOH), and KOH (as-deposited). The dark and lighter lines represent the experimental spectrum and the components resulting from deconvolution, respectively.

Summarizing, the KOH treatment removes the oxidized PbSe surface, which we tentatively identify with an oxide, hydrated oxide, and/or basic carbonate of Pb. Removal of this protective coating allows the KOH to gradually dissolve and reprecipitate PbSe to form larger crystals, probably via an Ostwald ripening mechanism. Since PbSe oxidizes fairly readily on the surface, even freshly formed PbSe will surface-oxidize again when exposed to air. However, the larger PbSe crystals formed by the KOH treatment will have a smaller surface-to-volume ratio and therefore relatively less oxide.

**NMR of TSC Samples before and after KOH Treatment.** Proton NMR can provide information on the hydrogen content of the nanocrystalline surface (no H is expected in the bulk). Proton NMR of the precipitates from the TSC solutions were carried out after drying the samples at high vacuum for at least a day. The residual proton spectra are shown in Figure 4. The highly structured line shapes were analyzed by deconvolution and their line compositions<sup>10</sup> are summarized in Table S2 (Supporting Information). Lines corresponding to the same type of protons are combined in the deconvolution. The spectrum of the TSC sample (Figure 4 (TSC)) before KOH treatment consists of four lines, corresponding to nonhydrated surface hydroxyl groups (at 1.3 and 2.8 ppm, 22% of the protons), residual water (at 5.3 ppm, 42% of the protons), and apparently protons exchanging {H<sub>2</sub>O–OH} between water and hydroxyl groups (at 4.4 ppm, 36% of the protons). Of particular note, since some of the hydroxyl groups are not hydrated (second column in Table S2), this means that the surface “oxides” contain hydroxyl groups. This also seems to be the case for the –OH exchanging with water (column 3 in Table S2), but in that case, it could be argued that the hydroxide might be merely dissociated surface water. We note that in our proton NMR experiments all hydrogens of rigid molecules on the surface

(9) Gautier, C.; Cambon-Muller, M.; Averous, M. *Appl. Surf. Sci.* **1999**, *141*, 157.

(10) Pizzanelli, S.; Kababya, S.; Frydman, V.; Landau, M.; Vega, S. *J. Phys. Chem. B* **2005**, *109*, 8029.

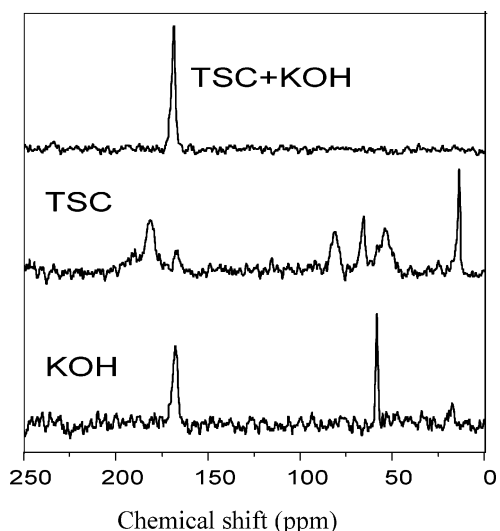


**Figure 5.** Room temperature  $^{13}\text{C}$  CPMAS spectra of PbSe precipitates (designations as in Figure 4).

are not detected. After the sample is heated at 200 °C for a period of 12 h, the four lines reduced in intensity: the  $-\text{OH}$  groups by 50%, the  $\{\text{H}_2\text{O}-\text{OH}\}$  protons shifting from 4.4 to 4 ppm, by 65%, and the water by about 45%; an overall loss was on the order of 50%. During the sample heating, the sample lost 2.1 mg and the residual sample weight was 154 mg. This overall loss of water indicates that there is about the same amount, ca. 2 mg, of water and  $-\text{OH}$  groups left in the sample. This allows us to make a rough estimate, based on the known  $\text{Pb}-\text{O}$  to  $\text{PbSe}$  from the XPS data, that about 25% of the oxidized Pb contains a detectable OH bond.

After the KOH treatment of a TSC sample (with 0.25 M KOH for 15 min) and vacuum drying for 1 day, the proton spectrum was significantly modified, as can be seen in Figure 4 (TSC + KOH) and in Table S2. Two downfield-shifted lines appeared at 6.3 and 8.4 ppm (15% and 14% protons, respectively), hydroxyl protons at 2.3 ppm (31%), water (only 15%), and  $\{\text{H}_2\text{O}-\text{OH}\}$  exchanging protons at 3.7 and 4.5 ppm (16% and 9%, respectively). After an additional heating of the sample at 200 °C overnight, the total intensity of the proton spectrum did not change significantly. Only the hydroxyl line became 2 times higher on account of the  $\{\text{H}_2\text{O}-\text{OH}\}$  protons. It seems that the KOH treatment removed most of the water coverage of the particles and, furthermore, created a significant amount of acid-type protons. The relative  $-\text{OH}$  and  $\{\text{H}_2\text{O}-\text{OH}\}$  coverage remained intact. However, an absolute comparison between this spectrum and the spectrum of the original TSC sample was not possible. A change in particle size after the KOH treatment could not be taken into account during data analysis. Residual adsorbed molecules on the particles do not contribute to our proton spectra, but could be detected by  $^{13}\text{C}$  NMR.

The  $^{13}\text{C}$  CPMAS NMR spectrum of a dried TSC sample is shown in Figure 5. The main lines are located at 14 and 180 ppm, originating from the residual lead acetate in the sample, and at 81, 66, and 54 ppm, partially originating from the sodium citrate and some residual ethanol used during sample preparation. An additional line at 168 ppm is an indication of the presence of some carbonate complex. The

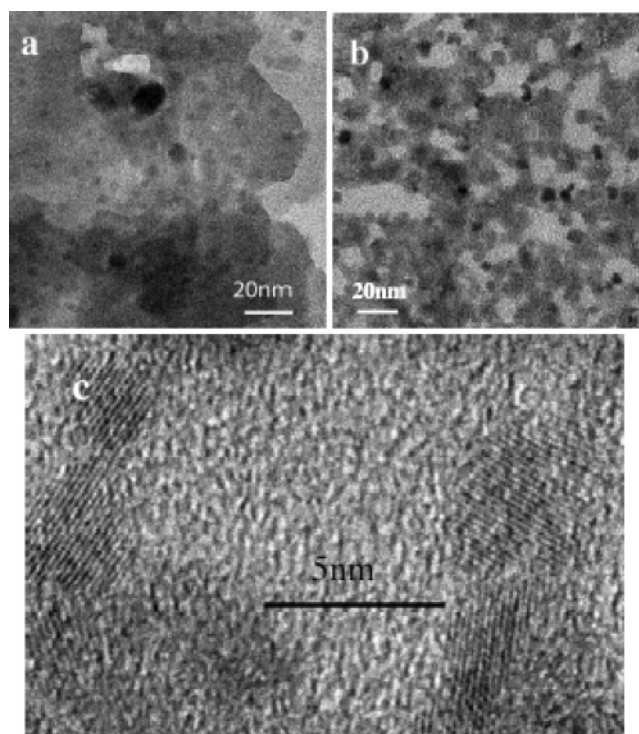


**Figure 6.** TEM micrographs of PbSe films as-deposited (a) using KOH as a complexing agent and after KOH treatment at two different magnifications ((b) and (c)).

carboxyl carbons of the citrate were not present in the sample. After the KOH treatment all acetate and citrate moieties were removed from the sample and only a carbonate line at 169 ppm remained.

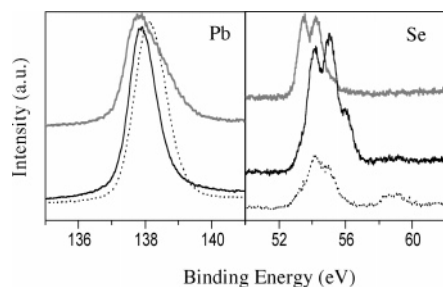
#### TEM of KOH Films before and after KOH Treatment.

Figure 6a shows a TEM image of a thin KOH film. While the PbSe crystal size is comparable (slightly smaller, ca. 4 nm, but including many smaller ones) to that of the TSC films, there is a clear difference in the structure of the films. The KOH films contain relatively widely spaced particles separated by large amounts of some amorphous matrix (this can explain the absence of an XRD pattern: the concentration of PbSe is low). In contrast to the TSC films, where we noted that what at first sight looked amorphous was by a change in the focal depth shown to be crystalline PbSe, the KOH film matrix remains featureless under varying focal depths. EDS analyses showed a  $\text{Pb}:\text{Se}$  ratio of 4 [the ratio varies considerably from sample to sample, reflecting a varying ratio between PbSe and the matrix; the value of 4, given here (a similar value is seen also in the XPS analysis; see below) is typical] in large areas of the film and a ratio equal to 19 in the matrix regions where there were only a few crystals present. It is therefore reasonable to assume, based on simple chemical considerations, that the matrix is a hydrated lead oxide, possibly also containing some basic  $\text{PbCO}_3$ .

After KOH treatment, TEM showed that much of the matrix has been removed. However, in contrast to the TSC films, the PbSe crystal size remained unchanged (Figures 6b and 6c).

#### XPS of KOH Films before and after KOH Treatment.

We first compare the XPS spectra of the as-deposited KOH films with the corresponding TSC films. (Figure 7). Decon-



**Figure 7.** XPS spectra of Pb (left) and Se (right) of KOH PbSe both as-deposited (dotted lines) and after KOH treatment (solid lines), together with the as-deposited TSC spectra from Figure 3 (gray lines).

olution of the broad Pb line of the KOH films into a PbSe low BE peak and a Pb–O high BE peak is quantitatively limited due to the significant overlap of the two lines (for this reason, only the total peak intensity is given in Table S1). However, the shift of the peak of the KOH film relative to the TSC film indicates an increase of Pb–O relative to PbSe. This increase can be correlated to Pb–O in the matrix. We can be a bit more quantitative by attributing all the Se to PbSe (this assumption holds reasonably well for the TSC film both before and after treatment, where the lower BE Pb concentration is approximately the same as the total Se concentration). With this assumption, the lower BE Pb would be 6.65 atom % (the same as the Se; see Table S1), leaving 22.1 atom % from the Pb–O.

The C spectra do not show any high BE carbonate carbon; therefore, the matrix does not contain appreciable amounts of carbonate. Also, the small carboxylate peak in the C spectrum of the TSC film is absent in the spectrum of the KOH film as expected.

The Pb:Se ratio in the KOH film (4.3) is much higher than that for the as-deposited TSC film (2.0) (Table S1), in agreement with the EDS analysis. The Se spectrum is unusual compared to that of the TSC film (we stress that this Se spectrum is reproducible for KOH-deposited films). There is only a very small signal at 53.3, which is the lower BE peak associated with PbSe. Instead, most of the Se signal is concentrated in a doublet corresponding to what we termed Se(Pb-ox). We know, from TEM, that there is PbSe in these samples. Thus, this Se(Pb-ox) is actually part of the oxidized surface of PbSe particles coating: it is not characteristic of Se–O bonds, which should be at a higher BE. This coating in the KOH films is different from that in the TSC films and will be discussed below. There is, however, some oxidized Se present in the KOH film, probably  $-\text{SeO}_x$ . Both O peaks (529.2 and 531.0 eV) are in the range of reported Pb oxides, associated here with the interparticle matrix. When the concentration of selenosulfate in the deposition solution was increased (see row 7 in Table S1), the ratio of Se to Pb increased somewhat as expected, but the overall distribution of the different chemical species was still similar to that of the original KOH films (row 5 in Table S1) and different from the TSC films.

This comparative study indicates that there is less PbSe and more Pb–O in the KOH films than there is in the as-deposited TSC films. Furthermore, Pb–O (not carbonate) makes up most of the matrix in the KOH films.

We note that the rationale for this study was to understand the difference in the response of TSC and KOH films to the KOH postdeposition treatment. Since the KOH treatment does not affect the crystal size of the KOH films, we were surprised to find that this treatment did have a strong effect on the XPS spectra and on the stoichiometry of the films. The Pb:Se ratio decreased from 4.3 (before treatment) to 1.2 (after) (see the XPS analyses in Table S1) and the Pb peak narrowed appreciably and moved a little toward lower BE. After the KOH treatment, the Se spectrum, apart from variations in intensities, did not change drastically; most of the Se–O was removed, the higher BE component of the Se(Pb-ox) was more clearly visible as a shoulder at ca. 56 eV, and the small signal at ca. 53 eV, which was visible as a very small shoulder on the as-deposited spectrum and is characteristic of the  $3d_{5/2}$  pure PbSe, became more pronounced. From the large change in stoichiometry we infer that most of the Pb–O part of the matrix was removed by the postdeposition treatment, but that the crystals were still covered with a KOH-resistant oxidation layer (to be discussed later).

**NMR of KOH Samples.** The proton spectrum of a KOH sample, after vacuum drying for a day, is shown in Figure 4 (KOH) and has a line structure resembling the KOH-treated TSC sample: a water line at 4.9 ppm (12% protons), a low field line at 6.3 ppm (54%), hydroxyl protons at 2.3 ppm (12%), and  $\{\text{H}_2\text{O}-\text{OH}\}$  exchanging protons at 3 and 4 ppm (11% each). In this case additional heating at 200 °C for 30 min removed almost all protons from the sample, reducing its weight by 2.8 mg and leaving only 20% total intensity, half  $-\text{OH}$  and half acid-type protons. The weight of the residual sample was 209 mg with  $<0.7$  mg of  $-\text{OH}$  and acid protons present. This presumably indicates that heating the sample removes the free and bound water from the matrix. The (water-free)  $-\text{OH}$  changed only slightly after this heating step and it is tempting to associate it with the surface of the PbSe nanoparticles in the matrix. The acid protons, which make up half of the total protons in the (nonheated as well as heated) samples, are most likely associated with the matrix since they form the bulk of the sample.

The  $^{13}\text{C}$  CPMAS NMR spectrum of a KOH sample is shown in Figure 5 (KOH). This spectrum consists of a carbonate line at 17 ppm and a line at 58 ppm probably coming from some residual ethanol used during sample preparation.

**High pH TSC Films.** To find out whether the difference between the TSC and KOH films is caused by the presence of citrate adsorbed at the crystal surfaces or a result of the high pH during deposition, TSC films were also grown at a high pH (pH 12 adjusted by adding KOH to the deposition solution). These films, like the KOH ones, do not exhibit crystal growth when treated with KOH after deposition. The Pb, Se, and O XPS spectra of the high pH TSC film are very similar to those of the KOH-deposited film (the semiquantitative results are given in the last row of Table S1). The only clear difference is the presence of the carboxylate C peak at 289.2 eV in the high pH TSC film. This demonstrates clearly that the difference between the

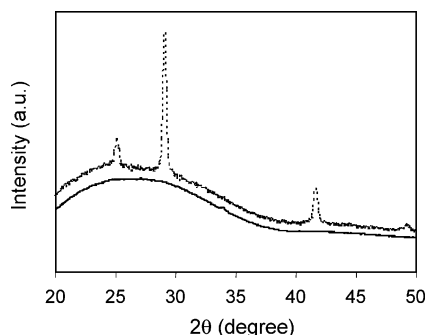


**Figure 8.** XRD of a KOH PbSe film as-deposited (lower spectrum). The spectrum after standard KOH treatment (0.25 M KOH for 15 min) is identical. The upper spectrum is for a KOH film after treatment with 3 M KOH for 70 min.

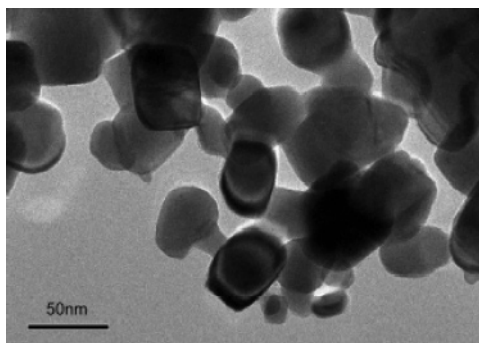


**Figure 9.** TEM micrograph of a KOH film after 70 min in 3 M KOH.

normal TSC (deposition pH < 11) and the KOH films is connected to the difference in the pH of the solution during precipitation and not with the presence of citrate.

**Treatment of KOH Films with KOH under More Aggressive Conditions.** Hydroxide is a strong complexant for Pb and PbSe can be dissolved by KOH under sufficiently aggressive conditions. Also, if KOH is added to a  $\text{Pb}^{2+}$  solution, the initial precipitate does not readily dissolve. If, however, the  $\text{Pb}^{2+}$  solution is added slowly to a KOH solution of sufficient concentration, then the lead does go into solution. This gives an idea of the importance of kinetics in these dissolution reactions. Thus, we expect that the oxide surface of the KOH film will eventually be dissolved if the treatment is made more aggressive and also that crystal growth might occur (assuming the PbSe does not dissolve faster than it grows). As anticipated, more aggressive KOH treatment (3 M KOH for 70 min, a treatment which destroys the TSC films) of the KOH films did result in crystal growth. While XRD showed no peaks for the as-deposited or normal KOH-treated KOH films, the aggressive KOH treatment resulted in sharp XRD peaks (Figure 8) and a network of large (tens of nanometers) PbSe crystals seen in TEM (Figure 9). The XPS spectra of KOH films treated in this way are very similar to those of normal KOH-treated TSC films with a Pb:Se ratio of 1.2 (data shown in Table S1).

**EXAFS Results.** The Pb or Se absorption edge step heights (not shown) are a measure of the total amount of Pb or Se, respectively, in each film. For the untreated samples (either from a TSC or from a KOH bath), the edge-step heights of Pb and Se were the same. However, based on the edge step height measurements, after treatment (in 0.25 M KOH for 10 min), both samples were found to lose Pb

relative to Se, but not in equal amounts. The TSC sample lost 30% more Pb than Se, while the KOH sample lost 65% more Pb than Se. The changes in the relative Pb and Se edge steps in the KOH sample before and after the KOH treatment confirm conclusions derived from XPS that there is relatively less PbSe and more Pb–O in the TSC films compared to the TSC films. Note that the fluorescence measurement, unlike XPS, is a bulk measurement of relative elemental composition.

EXAFS data were modeled by simulating the nearest neighbor environment of Pb and Se as Pb–O (Se–O) and Pb–Se (Se–Pb) bonds. The FEFF6 program<sup>11</sup> was used to generate theoretical photoelectron phase and amplitude functions to construct an EXAFS model for the local environments. Nonlinear least-squares fit of the EXAFS theory to the data was performed using the IFEFFIT package.<sup>12</sup> The coordination numbers, average distances, and their mean square disorders ( $\sigma^2$ ) were varied in the fits. The mean square disorder represents the total spread of bond-length deviations about the average distances. Physically reasonable constraints were applied to decrease correlations between fitting parameters. For example, the  $\sigma^2$  of the Se–O bond before and after KOH treatment in the KOH-prepared sample was constrained to be the same before and after the KOH treatment.

Figures 10–12 show EXAFS data and fits to Pb  $L_3$ -edge and Se K-edge. Numerical results are summarized in Tables S3–S6 (Supporting Information). Both visual examination of Figures 10 and 11 as well as the quantitative results of Tables S3 and S4 demonstrate that the coordination numbers of Pb–O and Se–O decrease and Pb–Se and Se–Pb increase after KOH treatment. The Pb–Se and Se–Pb coordination numbers of the treated samples approach 6, which is characteristic of the rock salt structure of bulk PbSe. This is consistent with the increasing stoichiometric PbSe content of the films found also by XPS.

Coordination numbers of Pb–O bonds reported in Tables S3–S6 suggest that the sample as-deposited from the KOH bath has a larger ratio of the number of Pb–O bonds to the number of Pb–Se bonds than the TSC sample. Again this is consistent with the XPS results and can be explained by the presence of a matrix containing Pb–O bonds.

EXAFS data obtained for Se K-edge in the KOH samples could not be analyzed by a simple two-component model assuming just Se–O and Se–Pb contributions, as for the TSC sample. Such difficulty could be caused by the presence of elemental Se in the KOH samples that is present as a colloid in solution and becomes incorporated into the film to some extent. Thus, the local environment of Se may have all three components: Se–O, Se–Se, and Se–Pb. The information content in the EXAFS data is limited by the relatively narrow data range (from 2 to 9  $\text{\AA}^{-1}$  in  $k$ -space and from 1.5 to 2.7  $\text{\AA}$  in  $r$ -space, corresponding to five relevant independent points in the data). Therefore, simultaneous refinement of the contribution of these bonds which

(11) Zabinsky, S. I.; Rehr, J. J.; Ankudinov, A.; Albers, R. C.; Eller, M. J. *Phys. Rev. B* **1995**, *52*, 2995.

(12) Newville, M. J. *Synchrotron Radiat.* **2001**, *8*, 322.

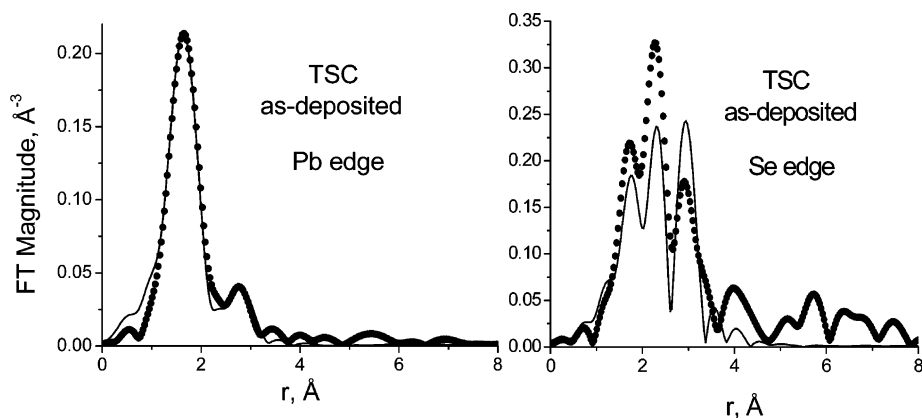


**Figure 10.** Fourier transform magnitudes of the  $k^2$ -weighted EXAFS data (filled circles) and fits (solid trace) of the TSC sample: Pb edge (left); Se edge (right).

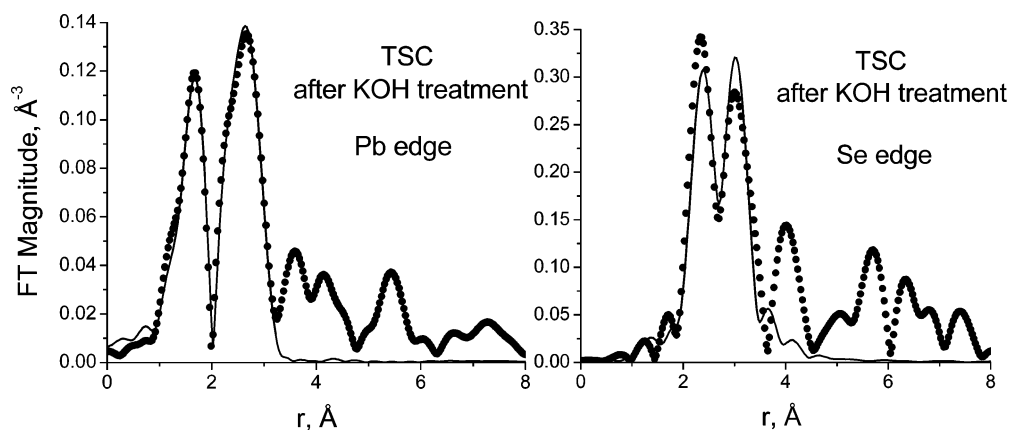


**Figure 11.** As Figure 10, but after sample was treated with KOH.

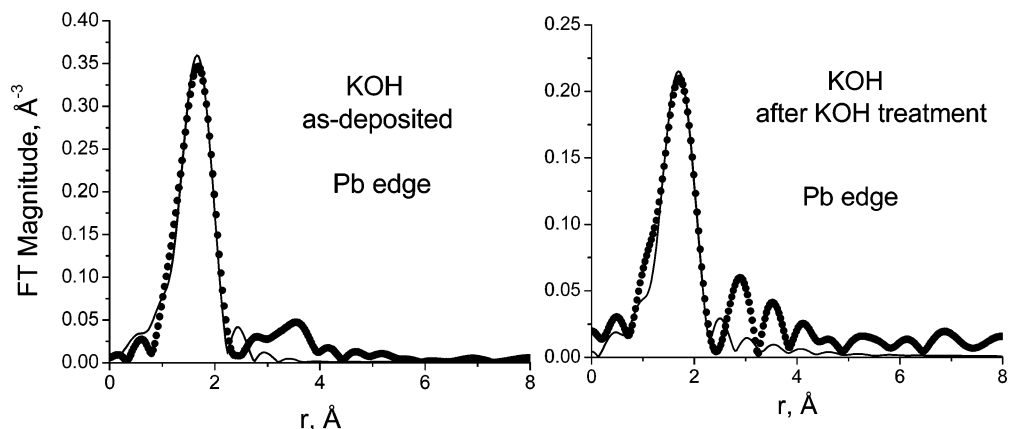


**Figure 12.** Fourier transform magnitudes of the Pb  $L_3$ -edge,  $k^2$ -weighted EXAFS data (filled circles) and fits (solid trace) of the KOH sample: as deposited (left) and KOH-treated (right).

requires a number of variables greater than 5 is not possible within the constraints of the present data quality.

**Model.** The fraction of atoms of a nanocrystal which are surface atoms increases greatly as the size decreases in the range of relevance here (several nanometers). This fraction depends on the shape of the crystal, but is of the order of one-fourth, one-third, and nearly one-half for 5, 4, and 3 nm crystals, respectively. XRD and/or TEM give an average crystal size of ca. 5 nm for the TSC films and ca. 4 nm or even less for the KOH films. TEM and HRTEM show that, for both films, many of the crystals tend to be elongated and <5 nm (TSC) or 4 nm (KOH) in at least one dimension (see Figure 6c); such a shape will result in a greater surface-

to-volume ratio than a sphere containing the same number of atoms.

For the TSC films, where the oxidized Pb XPS line is stronger than the Pb–Se line, and the Pb:Se ratio is 2, at least the first two layers of each crystal have to be oxidized and Se-depleted (assuming no separate phase exists). We have also compared “fresh” and “aged” (TSC) PbSe films and found, not surprisingly, that the percentage of oxidized Pb increases with aging (see column 1 in Table S1). This further shows that oxidation of the Pb is not necessarily limited to just the surface Pb. Oxidized surface Pb does not necessarily mean that there is no Se bonding to the same Pb. Chemisorbed water or hydroxyl groups are, in principle,

enough. Note that while in the initially oxidized films (row 1 in Table S1), Se is replaced by O (the Pb:Se ratio is 2), further air oxidation retains the Pb:Se ratio, but still results in a growth in the Pb–O-like XPS peak (and also a small amount of Se–O bonds).

The effect of the KOH treatment for both types of film is clearly to remove part of the oxidized Pb and, for the TSC films, to cause crystal growth. XPS analyses have been previously carried out on the effect of KOH solutions on the surface of epitaxial layers of PbSe.<sup>9</sup> It was shown that aqueous or ethylene glycol solutions of KOH removed surface PbO and SeO<sub>2</sub> but KOH in ethanol or isopropanol did not. It was suggested that PbO and SeO<sub>2</sub> were insoluble in the latter two solutions, hence their inactivity. We also find that (0.25 M) KOH in EtOH does not cause crystal growth in the TSC films, in contrast to aqueous solutions. This supports the role of KOH in dissolving an oxidized surface prior to crystal growth. In ref 9, the KOH treatment removed oxidized Se. In our case, the treatment caused the formation of such Se. (Note that we deal with nanoparticles and hence with surface properties which may differ from those of the epitaxial layers in ref 9.) There are various possibilities for this oxidized Se (SeO<sub>2</sub>, SeO<sub>3</sub><sup>2-</sup>, SeO<sub>4</sub><sup>2-</sup>): however, in all cases we would expect dissolution in the KOH (or even in water). It is probable that the KOH treatment activates the surface of the nanocrystals in such a way that the Se oxidizes in air subsequent to the treatment.

The crystal growth in the TSC films can be explained as follows: the KOH treatment dissolves part of the oxidized Pb (and less readily, PbSe), resulting in Ostwald ripening (dissolution of smaller crystals and redeposition on the larger ones). The elongated shape of the resulting crystals suggests that growth occurs by coalescence of several primary (5 nm) crystals in a row and thickening of this longer structure. The fact that the Pb:Se ratio decreases after the treatment means that there is some Se-free Pb compound in the as-deposited film (e.g., hydrated oxides or basic carbonates), presumably the oxidized coating on the nanocrystals, which dissolves in the KOH. If the KOH slowly dissolves PbSe in the Ostwald ripening mechanism, then we expect the presence of Se or Pb in the KOH solution to affect this dissolution. We found no increase in crystal size if a small amount of Pb (~5 mM lead acetate) is present in the KOH solution (0.25 M) irrespective of the treatment time. In contrast, the rate of increase in crystal size was accelerated in the presence of Na<sub>2</sub>SeSO<sub>3</sub> (≤2.5 mM) in the treatment solution. These data provide general support for the Ostwald ripening mechanism and its control by the availability of the minor component—the Se.

For the KOH films, the picture is not so clear. The high Pb:Se ratio in the as-deposited films (4.3) means that there is much more Se-free Pb species (the Pb–O matrix). The fact that the KOH treatment improves the stoichiometry to close to that of PbSe would imply that most of this matrix has been removed, as is clearly seen in the TEM image of Figures 6b and 6c. However, the normal KOH treatment has no effect on the individual PbSe crystals and also, as noted above, the chemical nature of the Se is quite different from that for “normal” PbSe. The Pb XPS signal of the normal

KOH-treated KOH film is characteristic of predominantly Pb–O, yet the Pb:Se ratio is close to stoichiometric. This could be explained by bonding of O to Pb which is also bonded to Se (not directly to Se, there is only a small amount of high BE Se characteristic of Se–O bonds). This same bonding could also explain the higher BE Se which predominates in these films: each surface Se is connected to four Pb–O species. As a simple consideration of the rock salt structure that PbSe shows, each Se one layer away from the surface is connected to one surface Pb–O species. This, at best, accounts for half the total Se. Therefore, more than a single layer of Pb(O)Se is needed to explain the more than 90% suppression of the low BE Se at ca. 53.4 eV. Consideration of many high-resolution TEM images of the KOH films after normal KOH treatment suggests that the 3–4 nm crystals may be very thin in many cases (low contrast of the lattice planes). This will further increase the surface-to-volume ratio, and therefore increase the measured fraction of the high BE Se and Pb lines.

While we cannot specify the exact nature of the two different surfaces of the TSC and the KOH films, which result in a large difference in reactivity to KOH, we can point to general differences in the two surfaces. Crystals in as-deposited TSC films have a surface which is dominated by Pb–O bonds, the O apparently substituting for Se. Correlating the oxidized Pb with the O concentration (Table S1), it is likely that there are two O atoms for every oxidized Pb (possibly related to Pb(OH)<sub>2</sub> or PbO·H<sub>2</sub>O). Oxidation of the Pb can continue further into the crystal, but with decreasing loss of Se. The KOH film crystals, both as-deposited and after the matrix has been removed by normal KOH treatment, are protected by a surface which contains Pb bonded to both O and Se, and this surface is very stable against attack by all but very concentrated alkali over a long period of time.

The high level of detail about the structure and compositional heterogeneity was only possible due to the combination of complementary techniques used in this study. For example, based on XPS data alone, we could not unambiguously distinguish chemical compositions of surface passivation and bulk. As our XPS results of the treated TSC samples show, there is a considerable amount of Se–O species in the TSC sample after KOH treatment and in the as-deposited KOH sample. From Se K-edge EXAFS results, we know that the bulk structure is PbSe rich and find no quantifiable Se–O contribution. Together, these techniques, XPS and EXAFS, allow us to propose the model where the Se–O layer is segregated at the surface, and the bulk phase is the nanoparticle PbSe. Additionally, the edge step height measurements, another bulk probe of composition, add credence to the assertions about the role of the KOH treatment in removing Pb–O. The NMR data indicate that the various surface oxides contain hydroxide groups, while the matrix of the KOH samples is dominated by acidic water groups (suggesting a positively charged surface). We cannot specify the exact nature of all the various oxides in this study, and in any case, it is possible that a surface stoichiometry occurs which does not exist in the bulk.

### Conclusions

CBD films of PbSe deposited from a citrate bath consisted of ca. 5 nm nanocrystals of PbSe with an oxidized (and Se-depleted) surface. Films deposited from (higher pH) KOH baths consisted of ca. 4 nm PbSe nanocrystals embedded in an amorphous lead oxide matrix. Aqueous KOH treatment of the citrate films resulted in a several times increase in crystal growth caused by dissolution of the surface Pb–O and Ostwald ripening of the PbSe by the KOH (which slightly solubilizes PbSe) and formation of a porous network of PbSe. The same treatment of the KOH-complexed films dissolved the oxide matrix but did not cause any crystal growth. The nanocrystals in these films were protected by a Pb(O)Se surface which was not readily soluble in KOH solution. Only by treating with very concentrated KOH for a long period of time was this surface layer removed and crystal growth then occurred. This work shows that what

may appear to be subtle differences in surface composition of nanocrystals can have major effects on their chemical properties.

**Acknowledgment.** We thank Ronit Popovitz-Biro for carrying out the high-resolution TEM and EELS measurements. This research was supported by the Israel Science Foundation. The Advanced Photon Source is supported by the U.S. Department of Energy, Basic Energy Sciences, Office of Science, under Contract No. W-31-109-ENG-38. A.I.F. acknowledges support of the U.S. Department of Energy Grant No. DE-FG02-03ER15477.

**Supporting Information Available:** Tables of XPS semiquantitative elemental compositions, proton NMR line compositions, and EXAFS results. This material is available free of charge via the Internet at <http://pubs.acs.org>.

CM060628U